Plasma sheath kinematics and some implications on the modeling of very low energy plasma focus devices

2012 Plasma Phys. Control. Fusion 54 095007

(http://iopscience.iop.org/0741-3335/54/9/095007)

Plasma Phys. Control. Fusion **54** (2012) 095007 (8pp) doi:10.1088/0741-3335/54/9/095007

Plasma sheath kinematics and some implications on the modeling of very low energy plasma focus devices

Felipe Veloso[1,2,3,5], **Ariel Tarifeño-Saldivia**[1,2,3], **Cristian Pavez**[1,2,3], **José Moreno**[1,2,3], **Marcelo Zambra**[1,2,3,4] **and Leopoldo Soto**[1,2,3]

[1] Comisión Chilena de Energía Nuclear, Casilla 188-D, Santiago, Chile
[2] Center for Research and Applications in Plasma Physics and Pulsed Power–P4, Santiago, Chile
[3] Facultad de Ciencias Exactas, Universidad Andres Bello, Av República 252, Santiago, Chile
[4] Universidad Diego Portales, Manuel Rodriguez Sur 415, Santiago, Chile

Received 4 January 2012, in final form 29 May 2012
Published 27 July 2012
Online at stacks.iop.org/PPCF/54/095007

Abstract
The kinematics of the plasma sheath in two very low energy plasma focus devices (∼70 and ∼300 J) is studied by means of non-perturbative optical diagnostics. Experiments are performed in deuterium at the filling pressure where neutron emission is maximum on each generator. In both devices, the sheath movement is monitored close to the anode surface, from where their thicknesses and their average propagation velocities are obtained. It is found that the sheath thicknesses are closer to or lower than 1 mm, which is significantly smaller than those measured in larger devices. Moreover, it is found that the sheaths remain attached for a period of time close to 20–30% of the quarter period of the discharge, and it coincides with estimations using theoretical models of sheath formation. These results suggest that the usual modeling tools used in plasma focus need further revision given that some discarded parameters such as plasma resistance and detachment time are important in very low energy devices, which is not necessarily true for high-energy devices. Some calculations and comparison with models are presented and discussed.

(Some figures may appear in colour only in the online journal)

1. Introduction

The plasma focus is a pulsed device where the current flowing through the plasma produces its own confinement magnetic field, resulting in a dense z-pinch column [1–3]. In these experiments, a plasma sheath is produced over an insulator surface after a pulsed discharge from a capacitor bank. This sheath detaches from the insulator and is accelerated along the axial direction of the electrodes. After reaching the open end of the coaxial electrode assembly, this sheath implodes in the radial direction, finally pinching onto the symmetry axis. This pinching effect produces a dense and hot z-pinch column, which has been widely studied in both basic plasma physics and applied research related to x-rays, ions and neutron sources (the latter, from fusion reactions when operated in deuterium or deuterium–tritium gas). It has been extensively reported that the appropriate pinching of a plasma and the radiation emission is in close relation to the appropriate formation of the plasma sheath and its movement prior to the pinching phase, i.e. the detachment, the axial and radial phases [4–7]. For this reason, there have been several experimental studies concerning the dynamics of the current sheath prior to the pinching phase in different gases; most of them having stored energies larger than 1 kJ in the plasma focus [8–16]. However, in the last decade there has been an increasing interest in studying such devices toward lower energies (lower than 1 kJ) for their potentiality to be used as portable devices even with repetitive operation [15–31] in different applications such as soil humidity measurements [24] and explosives and illicit material detection [32] among others. In addition to this, much effort has been made to understand the scaling laws of operation together with their similarities and differences

[5] Present address: Departamento de Fisica, Pontificia Universidad Catolica de Chile, Av Vicuña Mackenna 4860, Macul, Santiago, Chile.

Table 1. Electrical and load parameters of PF-50J and PF-400J.

	Electrical parameters					Load parameters (see figure 1(*a*))					
	C_0 (nF)	L_0 (nH)	V_{charge} (kV)	Stored energy (J)	Quarter period (ns)	D_2 pressure (mbar)	a (mm)	b (mm)	Z_{eff} (mm)	L_{ins} (mm)	R_{ins} (mm)
PF-50J	160	∼40	∼29	∼67	∼150	6	3	11	3.32	23.9	4.76
PF-400J	846	∼37	∼27	∼308	∼330	9	6	13	6.4	21	8

among the different ranges of stored energies that drive the plasma [33]. For these reasons, the experimental information regarding plasma parameters (such as breakdown, axial and radial sheath movement, sheath parameters, pinching and radiation emission among others) is extremely important for complementing knowledge of these very low energy plasma devices.

Additional to the experiments, the simulation models allow comparison among experimental results and plasma properties such as efficient energy transfer and induced voltage among many others. These models are mainly based on the snowplough effect of the plasma sheath during the axial and radial phases, using either a piston model for the sheath movement [34–38] or multiple finite two-dimensional elements resulting in a curved plasma sheath [39, 40]. However, all of these models were constructed comparing their results with the available data of larger energy devices (i.e. larger than 1 kJ). Regardless of the model to be used, the comparison with experimental results is crucial in order to test the applicability of such models in very low energy devices. There are some comparison tests for the radiation emission and sheath structure in sub-kJ devices published elsewhere [41, 42]. Nonetheless, they require some modifications to the load parameters (in [41]) or approximations to the sheath position (in [42]) in order to adjust the experimental results to the simulations. A possible explanation on the use of these modifications is that the models might need some corrections when operating in very low energy devices.

The optimization of plasma focus devices as a pulsed and portable neutron source for different applications, not only depends on the ability to change the main parameters of the generator (e.g. electrode design, operating pressure and repetition rate), but more crucial is the understanding of the physics behind these devices, in particular the low energy ones. There have been some reports regarding the variation of these parameters and their influence on the radiation emission [43–45]. Given the large quantity of possible parameter combinations for obtaining such an optimized neutron source, the use of comparative results and computer simulations seems mandatory. There is a well-known comparative study on high-energy devices [46], but as far as the authors are aware, there is a lack of such comparisons on smaller devices. In order to provide a further insight into the physics of very low energy plasma foci and to compare their kinematic properties this work concentrates on the plasma sheath movement prior to the pinch phase and the applicability of different models and commonly used approximations. The latter is performed using experimental measurements on two devices operating at ∼70 and ∼300 J using deuterium gas. These measurements were performed using non-perturbative optical plasma diagnostic methods. The latter discusses some implications of these results on the modeling of plasma foci. These results provide benchmarking data for deuterium-operated devices for neutron emission at very low energies and a guidance for improving simulations modeling of the discharges.

2. Experiments and results

The experiments were performed in the PF-50J [15–18] and PF-400J [7, 19, 20] devices. These generators were both designed and constructed in our lab, and they are quite similar in the capacitor bank arrangement, connections and spark-gap switching sections. The main differences among them are the bank capacitance and load section. They are characterized for being very low energy plasma focus devices with short quarter periods (∼30–70 J, ∼150 ns and ∼300–400 J, ∼310–330 ns, respectively). The electrical parameters of the devices are summarized in table 1. The load section of the generators consists of two concentric electrodes separated by an alumina insulator, inside a chamber filled with deuterium gas at a certain pressure. A common schematic diagram, useful for the load of both generators, can be seen in figure 1(*a*), whereas their parameters are included in table 1. The electrical diagnostics of the discharge are also similar in both generators. Voltages are monitored using resistive dividers, and current derivative signals are obtained using Rogowski coils. Typical current traces for both devices can be seen in figures 1(*b*) and (*c*). The neutron emission from each generator is measured using moderated ^{3}He-filled proportional counters arranged in the side-on direction [47–50] and monitored with scintillator–photomultiplier arrangements. The neutron yield obtained from the discharges is $\sim 3 \times 10^4$ n/shot for PF-50J at 6 mbar and $\sim 1.06 \times 10^6$ n/shot for PF-400J at 9 mbar. Further details on the neutron emission from each generator can be found elsewhere [18, 19, 49].

The kinematics of the plasma sheath is obtained by measuring the time-varying position of the plasma close to the anode surface (closer than $0.1a$; where a is the anode radius). In the PF-50J device, this information is obtained from several interferometric images at different times from different shots under similar conditions. These images are taken using a frequency-doubled Nd : YAG laser ($\lambda = 532$ nm, 8 ns pulsewidth) with Mach–Zehnder interferometry. The images are acquired using a CCD camera (Electrim EDC-1000N). The CCD size is 4.7×3.5 mm^2 and the resolution is 658×496 pixels. To produce the image in the interferometer, a magnification $m = 0.384$ is used, thus a resolution of

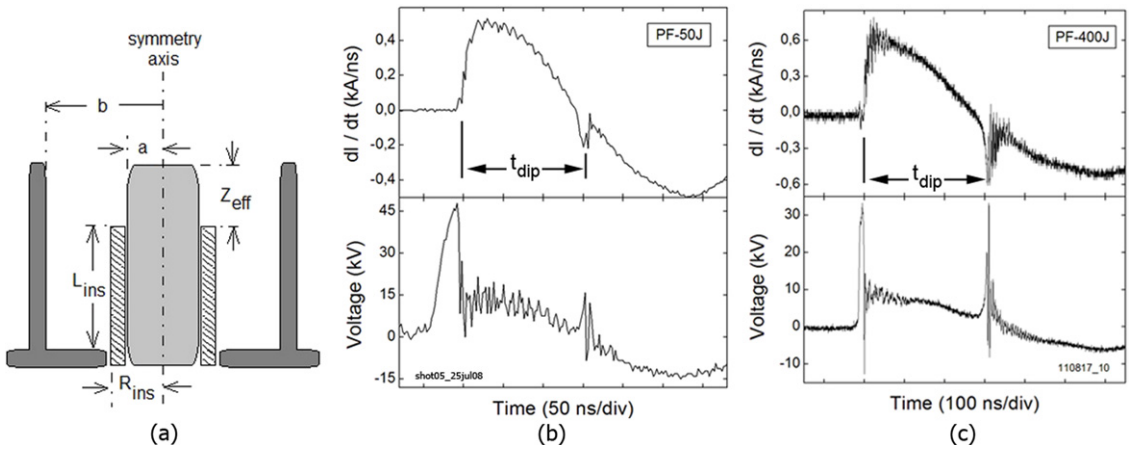

Figure 1. (*a*) Schematic diagram of the electrodes used in both PF-50J and PF-400J. (*b*), (*c*) Typical current derivative and voltage traces for PF-50J and PF-400J, respectively. The time to dip (t_{dip}) is indicated.

0.019 mm/pixel is obtained. Density measurements from these images are outside the scope of this paper, and they can be found elsewhere (together with sequences of interferograms for both axial and radial phases) [16, 49]. The plasma sheath position measurements are taken from the position of the perturbation on the interferogram due to the plasma refraction close to the anode surface (at ∼0.25 mm from it). The position of the plasma sheath is averaged from the measures in both halves of each image according to the symmetry axis. This position during each movement phase (axial and radial) for the PF-50J device is shown in figure 2. In this case, the vertical error bars correspond to the tolerance for the position of the plasma sheath, and are assigned directly from the refractivity observations on the interferograms, while the horizontal ones are given by the temporal width of the laser pulse.

In PF-50J, the statistical analysis of electrical signals indicates that the mean time to dip is 156 ± 1 ns with a standard deviation of ∼8 ns taken from a total of 63 shots. The time to dip (t_{dip}) corresponds to the period lasting from the breakdown in the load to the minimum in the dI/dt dip, as shown in figure 1. The measurements of the position in the axial phase (figure 2(*e*)) were analyzed by approximating the movement to a constant velocity using a linear model and a weighted least-squares. Even though observations indicated that propagation velocities change along each phase within certain ranges, constant mean values are considered as characteristic values useful for comparison purposes. Moreover, the linear model approximation provides correlation coefficients larger than 0.92 indicating that the changes in velocity do not strongly affect the characteristic features of the sheath kinematics. It is concluded that the plasma has a mean axial velocity of $(3.9 \pm 0.5) \times 10^4$ m s^{-1}. In addition, the thickness of the plasma sheath has a typical value of 0.2 mm. The linear model also shows that breakdown, sheath formation and detachment from the insulator surface last around 30 ns after the start of the discharge. After detachment, the axial transit time is ∼70 ns. The radial transit starts close to 50 ns before the dip and lasts ∼40 ns. The mean implosion velocity during the radial phase is $(5.2 \pm 0.5) \times 10^4$ m s^{-1}, and the maximum implosion velocity is estimated to be around 7.8×10^4 m s^{-1}. The radial transit time could seem proportionally too long when compared with Mather-type mid-energy microsecond-long plasma foci. But in those cases, most of the time is consumed during the axial phase, which is not necessarily the case of hybrid-type plasma foci such as PF-50J and PF-400J.

In contrast to PF-50J, the plasma sheath kinematics of PF-400J is measured shot to shot using a different diagnostic method for the sheath movement similar to those described in [51, 52] since laser probing was not available at the time of this experimental campaign. In this case, an optically magnified image of the load is focused onto a screen, where five optical fibers are located. These fibers are arranged in the image plane in such a way to measure the light emission from the plasma sheath during its movement close to the anode during the axial phase. Both lens and optical fibers are located outside the vacuum chamber. From the signals of the optical fibers, a position–time plot is made, from where the linear fit provides the average axial speed and the detachment time. An actual picture of the diagnostic arrangement, together with optical setup parameters and the linear fit of a sample shot can be seen in figure 3. The position of optical fibers avoids misinterpretation from the light emitted in the same line-of-sight, since no plasma lies on it before the passage of the sheath. The optical fibers have a core diameter of 1 mm which, together with the optical magnification of the system $M \sim 4$, provides a spatial resolution of ∼0.25 mm in the object plane (load) with a depth-of-field of ∼0.7 mm. For the radial movement of the plasma, this diagnostic only provides the time when this phase begins locating an optical fiber monitoring the anode corner. The average radial speed is obtained using also the pinching time obtained from the current derivative signal. The fibers are coupled to fast photodiode detectors (10 ns both rise and fall times) providing temporally resolvable signals on the scope, which are related to the position of the fiber in the object plane. Whenever possible, the temporal full-width at half-maximum (FWHM) of the two closest-to-insulator optical fiber signals is also measured (depending on the signal-to-noise ratio), from where the initial plasma sheath thickness is estimated. Further details on the diagnostic technique are described elsewhere [53]. The measured velocities, detachment time and thickness

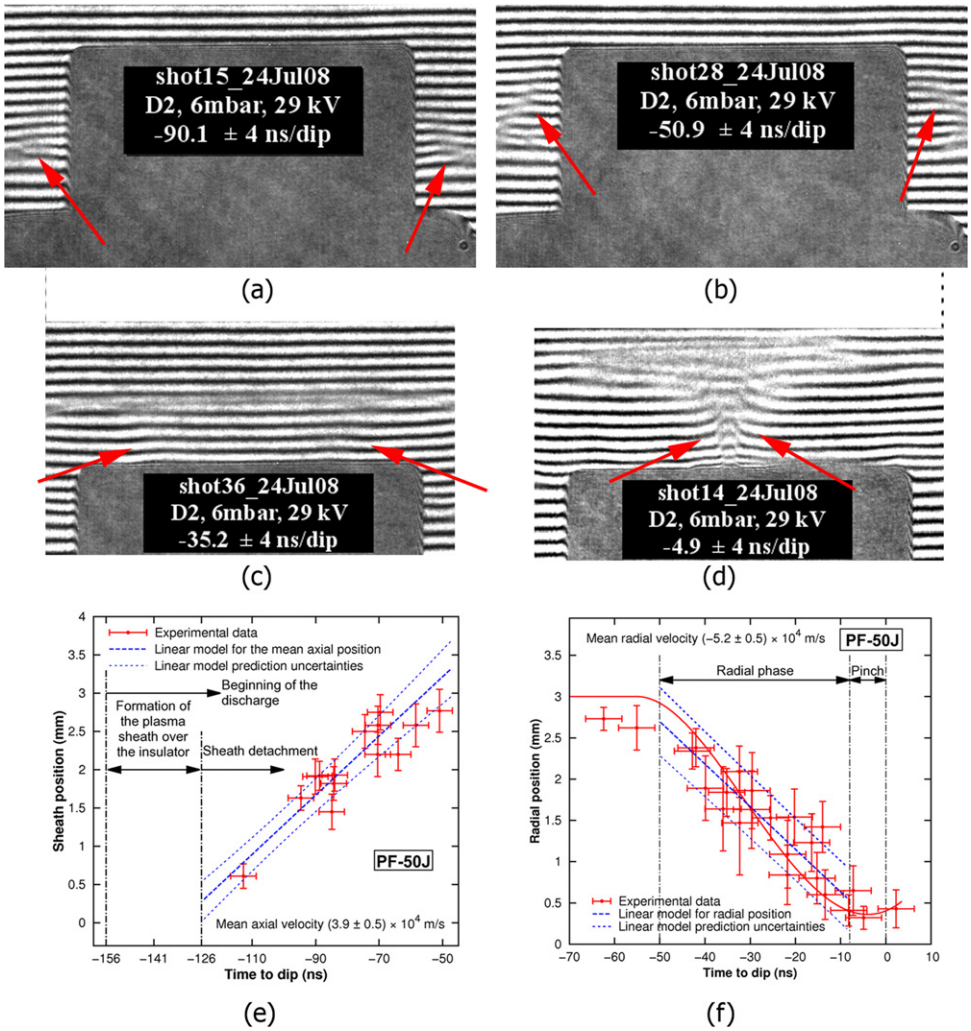

Figure 2. Measurement of the plasma sheath kinematics in PF-50J [49]. Interferograms of the movement during the axial phase (*a*), (*b*), during the radial phase (*c*) and pinching (*d*) where arrows indicate the sheath position. In (*e*) and (*f*), the plasma sheath position versus time is plotted taking several different shots. Time means the dip time in the current derivative signal.

of the sheath are included in figures 3(*c*)–(*f*). On this device, the mean time to dip is (314±7) ns, and the transit times for the plasma sheath in the PF-400J device are ∼140 ns and ∼75 ns for the axial and radial phases, respectively.

The experimental measurements of figures 2 and 3 show the plasma sheath kinematics during the axial and radial phases. It is interesting to point out that the measured axial speeds are nearly $4 \times 10^4\,\mathrm{m\,s^{-1}}$ for both fast and very low energy generators, which is nearly half of the usual values of $\sim 10^5\,\mathrm{m\,s^{-1}}$ observed in large energy devices, but within the range reported in [54]. Similarly, the average radial speed measurements indicate values in the range $(5\text{–}7) \times 10^4\,\mathrm{m\,s^{-1}}$, which are also nearly half of those of larger devices [46, 55] and lower than the range of [54]. Despite these differences from larger devices, the experimentally measured speeds of the sheath are in close agreement with those obtained using the snowplough model for the plasma movement in plasma focus discharges [35, 41, 56], as shown in table 2. Furthermore, the differences in these values when compared with larger devices are not so large given the orders of magnitude in energy difference with large devices. Additionally, the ratio of the plasma sheath velocities among the axial and radial phases remains similar with any plasma focus operated in deuterium. These observations provide further support to the idea of scalability in plasma focus devices [3, 33]. In PF-400J, the average radial speed is considered up to a final radius of $0.12a$, according to previous measurements from many devices and the scaling laws obtained for plasma focus [3, 16, 33, 56].

On the other hand, it can be seen (in both generators) that the plasma sheath detaches from the insulator surface in the axial phase after a certain time after the current starts flowing through the load (∼30 ns in PF-50J and ∼110 ns in PF-400J). This time period is defined as the detachment time and it is considered as the time when the center of the sheath is separated from the insulator by half of the measured thickness. Prior to this time, the plasma sheath is formed from the ionization of the background gas without moving and remaining attached over the insulator surface. This observation has also been made using optical diagnostics in a ∼6 kJ device using hydrogen [29] and deuterium [8] and evidenced in neon on a 3.3 kJ device [57], and additionally, on PF-400J itself using electrical diagnostic analysis (i.e. without using images) [7]. It should be

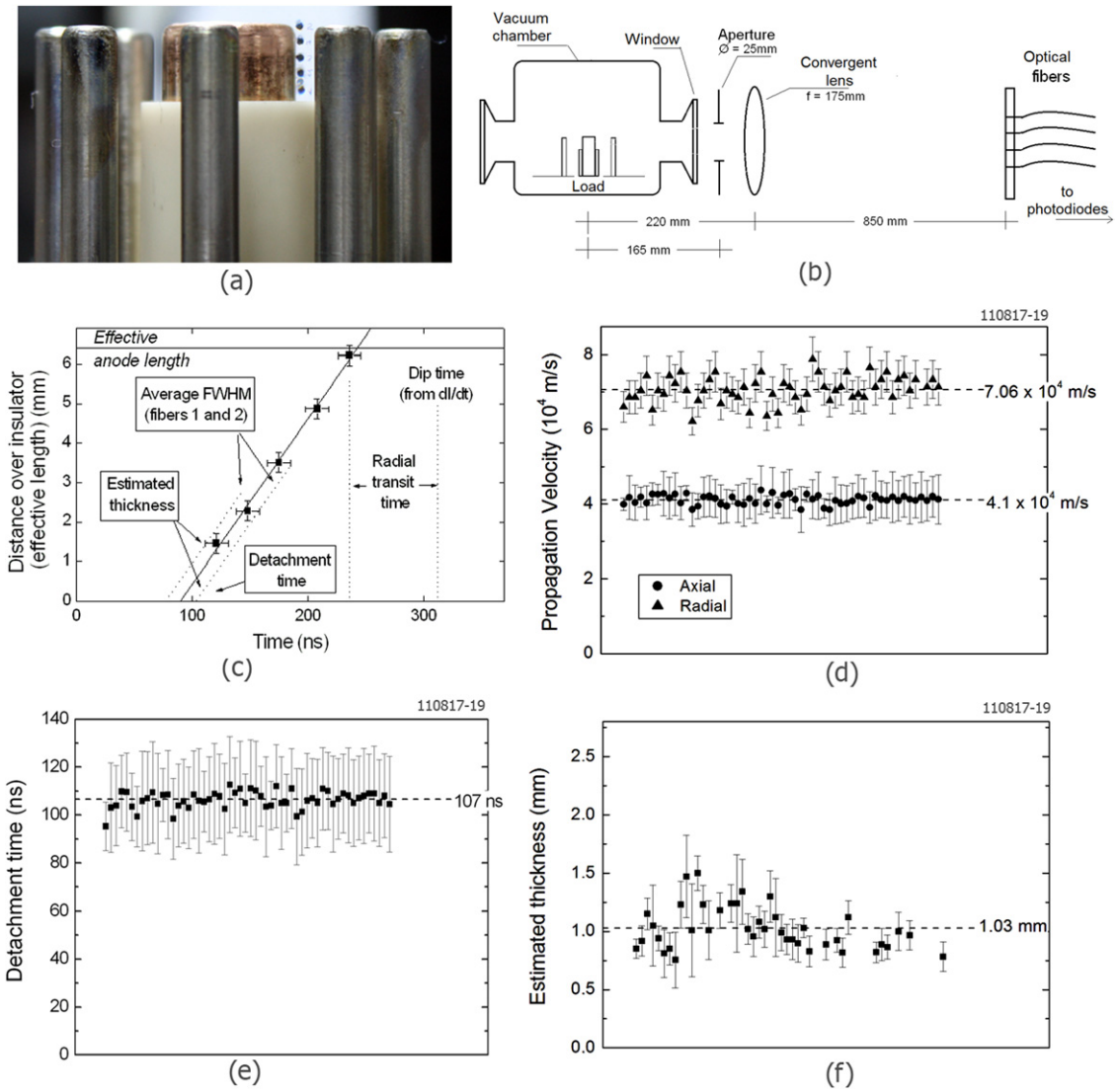

Figure 3. (*a*) Actual photograph where the image of the optical fibers (core + jacket) can be seen next to the anode. (*b*) Optical schematic setup for the diagnostic technique [53]. (*c*) Measurement of a sample shot. Plasma parameters obtained from several shots using the optical fiber data regarding (*d*) propagation velocities, (*e*) detachment time and (*f*) estimated initial thickness. Each point on (*d*), (*e*) and (*f*) represents an independent shot. Average values of each parameter are included.

Table 2. Comparison of some parameters of the plasma sheath among devices with different stored energies.

	PF-50J (at 67 J)	PF-400J (at 310J)	∼6 kJ ([8, 9])	POSEIDON ([46]) (at 500kJ)
Detachment time (ns)				
Measured	∼30	107	400	Not
	∼20% $T_{1/4}$	∼30%$T_{1/4}$	∼15% $T_{1/4}$	measured
Model [58, 59]	30	110	Thickness	800
(using measured Δ)			not available	
Average speed (m s^{-1})				
Measured	Axial: 3.9×10^4	Axial: 4.1×10^4	Axial: $(4-6) \times 10^4$	Axial: $\sim 1 \times 10^5$
	Radial: 5.2×10^4	Radial: 7.1×10^4	Radial: Not measured	Radial: 1.5×10^5
Snowplough model	Axial: 3.5×10^4	Axial: 3.5×10^4	Axial: 5.2×10^4	Axial: 1.6×10^5
	Radial: 7.5×10^4	Radial: 8.6×10^4	Radial: 6.0×10^4	Radial: 2.1×10^5
Resistance (Ω) ($\eta = \eta_{Spitzer}$, $T_e = 2$ eV)				
Detachment	0.71	0.067	0.01 (*)	0.0009
(after (1))	143% $(L_0/C_0)^{1/2}$	32% $(L_0/C_0)^{1/2}$	Not available	5.6% $(L_0/C_0)^{1/2}$
Axial phase	0.19	0.02	0.0015 (*)	0.0002
(after (2))	38% $(L_0/C_0)^{1/2}$	9.6% $(L_0/C_0)^{1/2}$	Not available	1.3% $(L_0/C_0)^{1/2}$

Note: (*) Calculated in [8] after electrical considerations. In the axial phase, the value is averaged over time.

pointed out that this time is not negligible when compared with the quarter period of each generator. The sheath thickness has average values of ∼0.2 mm (PF-50J) and ∼1.0 mm (PF-400J). In the case of PF-400J, the sheath thickness of ∼1 mm could be overestimated due to the ∼20–30 ns FWHM measured from the signals, which is close to the resolution of the photodiodes. In any case, the measured thicknesses in both devices are considerably lower than the usual centimeter range thickness measured in larger energy devices [10, 46].

3. Implications of sheath parameters in models

The movement of the deuterium plasma sheath is studied in two very low energy plasma focus devices, which operate at 67 J (PF-50J) and 308 J (PF-400J) with neutron yields of $\sim 10^4$ n/shot and $\sim 10^6$ n/shot, respectively. The kinematics of the plasma sheath is measured using optical diagnostics that do not perturb it while measuring. The results show that the sheath begins its movement after a certain period of time after the current starts flowing through the load. This observation has also been made previously in other devices, but surprisingly it is not included in the usual modeling of plasma focus [35–40]. The reason could be either for simplicity, or for considering it negligible when compared with the quarter of period of the discharge usually in the microsecond range, or for time compensation produced by using different electrode dimensions (particularly, the effective anode length) in the simulations. However, the experiments presented here are characterized by their shorter quarter period of hundreds of nanoseconds and shorter effective anode length (in addition to their very low stored energies). Hence, this attachment time is significant in the calculation of how the plasma sheath moves along the effective length of the anode. A similar situation can be described for experiments on hydrogen (at 120 J [29]), neon (at 3.3 kJ [57]) or deuterium (at 6 kJ [8]) reported elsewhere. Particularly, the simulations of PF-400J presented in [41] using the Lee model code [34, 35] were able to compute the neutron yield as a function of pressure within reasonable agreement. But these numerical simulations required adjustments on both the capacitor bank and electrode parameters in order to fit the experimental current waveform properly. The inclusion of the attachment time in the simulations should enhance the accuracy of the simulation, which could be proved by adding the necessary modifications on the code (which are certainly beyond the scope of this paper). The measured time when the plasma remains attached to the insulator could be compared with some of the available models for the formation of the plasma sheath in plasma focus devices. Some of these models are given in [58, 59], where the ionization and lift-off times have been analytically estimated. The summation of these times is taken as the detachment time. For these computations, the measured thicknesses of the sheath on the PF-50J and PF-400J devices are used and the results are included in table 2. It is interesting to point out that the analytical calculations are in very close agreement with the experimental values, demonstrating that the prediction capability is indeed possible even in these very low energy devices.

The scaling laws state that the energy stored in the capacitor bank of an operative plasma focus can be decreased as long as the electrode dimensions decrease properly. If these scaling laws are obeyed, the plasma parameters such as density and temperature remain similar among devices, regardless of the device energy [3, 33]. In particular, the anode radius a should be chosen in such a way as to fulfill the scaling parameters accordingly. The dimension of the anode radius certainly influences the radius of the insulator that covers it. In very low energy devices, such as the PF-400J and PF-50J devices, the small diameters of both anode and insulator, together with the measurements of sheath thickness, imply an important feature for plasma resistance when compared with larger energy devices. The resistance of the plasma sheath can be calculated from the following relations:

$$\frac{R}{\eta} = \begin{cases} \dfrac{L_{\text{ins}}}{\pi(\Delta^2 + 2R_{\text{ins}}\Delta)} & \text{at detachment} \quad (1) \\ \dfrac{\ln(r_{\text{out}}/r_{\text{in}})}{2\pi\Delta} & \text{axial phase} \quad (2) \\ \dfrac{z_{\text{pinch}}}{\pi r_{\text{pinch}}^2} \approx \dfrac{6.37}{a} & \text{at pinching} \quad (3) \end{cases}$$

where R and η are the plasma resistance and resistivity, respectively. Δ is the sheath thickness and r_{in} (r_{out}) is the inner (outer) radius of the plasma with limiting value on the anode (cathode) radius. In equation (3), the approximations on the height $z_{\text{pinch}} = 0.8a$ and the pinch radius $r_{\text{pinch}} = 0.12a$ are used [3, 56]. Even though this paper is not centered on the pinch phase, it is worthwhile to mention the resistance differences on the pinch phase given by the anode radius (which is related to the device energy according to the scaling laws). This observation could imply differences in the pinch stability, as mentioned in [33], and a proportionally extended radial transit time mentioned in the previous section. Using these relations, the differences in resistance among different devices are much more clear, since it is expected that the plasma temperature (and consequently, the resistivity) on each phase does not show significant variation on the different devices [58, 59]. The insulator dimensions, the sheath thickness and the anode radius in very low energy devices are considerably lower than those in larger energy devices. Table 2 shows the calculations for plasma resistance using the measured values for the PF-50J and PF-400J devices. For the sake of comparison, table 2 also includes similar calculations for two other devices; the high-energy device POSEIDON [46] operating at 500 kJ, and a low-energy device operating at 6 kJ [8]. In all cases, the Spitzer resistivity in a 2 eV fully ionized deuterium plasma is used. Even though other resistivity expressions can be used instead, the differences in plasma resistance among devices will be maintained in the same way. Additionally, these values are compared with the external circuit impedance $(L_0/C_0)^{1/2}$ when available. It can be seen that the plasma resistance (using the Spitzer resistivity on a fully ionized deuterium plasma) is comparable to and even larger than the circuit impedance, during the attachment and axial phase for very low energy devices. The same is not necessarily true for devices having stored energies larger than

1 kJ. This means that a time-varying plasma resistance should be carefully evaluated if it is intended to be neglected during modeling of very low energy devices, as is usually done for larger energy devices.

The study of plasma sheath movement along the axial and radial phases is important in order to provide a full picture of the plasma focus phenomena. In the case of very low energy devices (stored energies <1 kJ), the results show that the plasma sheath moves at speeds comparable to larger energy devices, in spite of the orders of magnitude of difference in energy. However, the lower operating energy (which leads to reduced load sizes) produces thinner plasma sheaths in the experiments, which imply considerations on the plasma resistance. The observed kinematics on ∼70 and ∼300 J operating plasma foci provide further support and knowledge to the scaling and modeling of very low energy plasma foci, which should be considered for future design and performance optimization of these kinds of portable devices.

Acknowledgments

This work is supported by the 1110940 project. The authors are also grateful to Mr Patricio San Martin for his valuable technical support, to Mrs Karla Cubillos for language reviewing and to Mr Victor Santibañez and Mr Benjamin Soto for their assistance during acquisition of some of the data.

References

[1] Mather J W 1965 *Phys. Fluids* **8** 366
[2] Filippov N V, Filippova T I and Vinogradov V P 1962 *Nucl. Fusion Suppl.* **2** 577
[3] Soto L 2005 *Plasma Phys. Control. Fusion* **47** A361
[4] Zakaullah M, Waheed A, Ahmad S, Zeb S and Hussain S S 2003 *Plasma Sources Sci. Technol.* **12** 443
[5] Ahmad S, Hussain S S, Sadiq M, Shafiq M, Waheed A and Zakaullah M 2006 *Plasma Phys. Control. Fusion* **48** 745
[6] Kies W 1986 *Plasma Phys. Control. Fusion* **28** 1645
[7] Veloso F, Pavez C, Moreno J, Galaz V, Zambra M and Soto L 2012 *J. Fusion Energy* **31** 30
[8] Tou T Y, Lee S and Kwek K H 1989 *IEEE Trans. Plasma Sci.* **17** 311
[9] Tou T Y 1995 *IEEE Trans. Plasma Sci.* **23** 870
[10] Bruzzone H and Grondona D 1997 *Plasma Phys. Control. Fusion* **39** 1315
[11] Bruzzone H and Martinez J F 2001 *Plasma Sources Sci. Technol.* **10** 471
[12] Bhuyan H, Mohanty S R, Neog N K, Bujarbarua S and Rout R K 2003 *Meas. Sci. Technol.* **14** 1769
[13] Al-Hawat S 2004 *IEEE Trans. Plasma Sci.* **32** 764
[14] Aghamir F M and Behbahani R A 2011 *J. Appl. Phys.* **109** 043301
[15] Moreno J, Silva P and Soto L 2003 *Plasma Sources Sci. Technol.* **12** 39
[16] Tarifeño-Saldivia A, Pavez C, Moreno J and Soto L 2011 *IEEE Trans. Plasma Sci.* **39** 756
[17] Silva P, Soto L, Moreno J, Silvestre G, Zambra M, Altamirano L, Bruzzone H, Clausse A and Moreno C 2002 *Rev. Sci. Instrum.* **73** 2583
[18] Soto L, Silva P, Moreno J, Zambra M, Kies W, Mayer R E, Clausse A, Altamirano L, Pavez C and Huerta L 2008 *J. Phys. D: Appl. Phys.* **41** 205215
[19] Silva P, Moreno J, Soto L, Birstein L, Mayer R E and Kies W 2003 *Appl. Phys. Lett.* **83** 3269
[20] Zambra M, Silva P, Pavez C, Pasten D, Moreno J and Soto L 2009 *Plasma Phys. Control. Fusion* **51** 125003
[21] Soto L, Pavez C, Moreno J, Barbaglia M and Clausse A 2009 *Plasma Sources Sci. Technol.* **18** 015007
[22] Pavez C and Soto L 2010 *IEEE Trans. Plasma Sci.* **38** 1132
[23] Verma R, Rawat R S, Lee P, Krishnan M, Springham S V and Tan T L 2010 *IEEE Trans. Plasma Sci.* **38** 652
[24] Milanese M, Moroso R and Pouzo J 2003 *Eur. Phys. J.* D **27** 77
[25] Rout R K, Mishra P, Rawool A M, Kulkarni L V and Gupta S C 2008 *J. Phys. D: Appl. Phys.* **41** 205211
[26] Shukla R, Sharma S K, Banerjee P, Das R, Deb P, Prabahan T, Das B K, Adhikary B and Shyam A 2010 *Rev. Sci. Instrum.* **81** 083501
[27] Verma R, Roshan M V, Malik F, Lee P, Lee S, Springham S V, Tan T L, Krishnan M and Rawat R S 2008 *Plasma Sources Sci. Technol.* **17** 045020
[28] Verma R, Rawat R S, Lee P, Springham S V, Tan T L, Roshan M V and Krishnan M 2009 *J. Plasma Fusion Res. Ser.* **8** 1283
[29] Hassan S M *et al* 2006 *Plasma Sources Sci. Technol.* **15** 614
[30] Barbaglia M, Bruzzone H, Acuña H, Soto L and Clausse A 2009 *Plasma Phys. Control. Fusion* **51** 045001
[31] Barbaglia M, Soto L and Clausse A 2012 *J. Fusion Energy* **31** 105
[32] Gribkov V A, Latyshev S V, Miklaszewski R A, Chernyshova M, Drozdowicz K, Wiacek U, Tomaszewski K and Lemeshko B D 2010 *Phys. Scr.* **81** 035502
[33] Soto L, Pavez C, Tarifeño A, Moreno J and Veloso F 2010 *Plasma Sources Sci. Technol.* **19** 055017
[34] Lee S 1984 *Radiations in Plasmas* vol II, ed B E McNamara (Singapore: World Scientific) pp 978–87
[35] Lee S 2010 *Radiative Dense Plasma Focus Computational Package:* RADPF http://www.intimal.edu.my/school/fas/UFLF/
[36] Gonzalez J, Clausse A, Bruzzone H and Florido P 2004 *IEEE Trans. Plasma Sci.* **32** 1383
[37] Gonzalez J, Brollo F and Clausse A 2009 *IEEE Trans. Plasma Sci.* **37** 2178
[38] Moreno C, Bruzzone H, Martinez J and Clausse A 2000 *IEEE Trans. Plasma Sci.* **28** 1735
[39] Moreno C, Casanova F, Correa G and Clausse A 2003 *Plasma Phys. Control. Fusion* **45** 1989
[40] Casanova F, Moreno C and Clausse A 2005 *Plasma Phys. Control. Fusion* **47** 1239
[41] Lee S, Saw S H, Soto L, Springham S V and Moo S P 2009 *Plasma Phys. Control. Fusion* **51** 075006
[42] Casanova F, Tarifeño-Saldivia A, Veloso F, Pavez C, Clausse A and Soto L 2012 *J. Fusion Energy* **31** 279
[43] Tarifeño-Saldivia A and Soto L 2012 Neutron emission and optimization of a tabletop plasma focus operated at tens of joules *Phys. Plasmas* submitted
[44] Beg F N, Zakaulah M, Nisar M and Murtaza G 1992 *Mod. Phys. Lett.* B **6** 593
[45] Woo H, Chung K and Lee M 2004 *Plasma Phys. Control. Fusion* **46** 1095
[46] Herold H, Jerzykiewicz A, Sadowski M and Schmidt H 1989 *Nucl. Fusion* **29** 1255
[47] Moreno J, Birstein L, Mayer R E, Silva P and Soto L 2008 *Meas. Sci. Technol.* **19** 087002
[48] Moreno J, Tarifeño-Saldivia A and Soto L 2010 *AIP Conf. Proc.* **1265** 505
[49] Tarifeño-Saldivia A 2011 Experimental study of a tens of joules small fast plasma focus discharge emitting neutrons *PhD Thesis* Universidad de Concepcion (In Spanish) (available at http://pppp.cl/descarga/ATarifeno_PhDTesis_V0.pdf)

[50] Tarifeño-Saldivia A, Mayer R E, Pavez C and Soto L 2011 Methodology for the use of proportional counters in pulsed fast neutron yield measurements arXiv:1110.2500v1
[51] Serban A and Lee S 1995 *Rev. Sci. Instrum.* **66** 4958
[52] Mahe L 1996 Soft x-rays from compact plasma focus *PhD Thesis* Nanyang Technological University (available at http://www.plasmafocus.net/IPFS/phdtheses/liumahe/Liu%20Mahe.htm)
[53] Veloso F, Moreno J, Pavez C, Tarifeño-Saldivia A, Zambra M and Soto L 2012 Non-intrusive plasma diagnostic for measuring sheath kinematics in plasma focus discharges *Meas. Sci. Technol.* **23** 087002
[54] Bernard A *et al* 1998 *J Moscow Phys. Soc.* **8** 93
[55] Gribkov V A, Bienkowska B, Borowiecki M, Dubrovsky A V, Ivanova-Stanik I, Karpinski L, Miklaszewski R A, Paduch M, Scholz M and Tomaszewski K 2007 *J Phys. D: Appl. Phys.* **40** 1977
[56] Lee S and Serban A 1996 *IEEE Trans. Plasma Sci.* **24** 1101
[57] Zhang T, Lin X, Chandra K A, Tan T L, Springham S V, Patran A, Lee P, Lee S and Rawat R S 2005 *Plasma Sources Sci. Technol.* **14** 368
[58] Bruzzone H and Vieytes R 1993 *Plasma Phys. Control. Fusion* **35** 1745
[59] Bruzzone H, Acuña H and Clausse A 2007 *Plasma Phys. Control. Fusion* **49** 105